Silver behaviour along the salinity gradient of the Gironde Estuary

Laurent Lanceleur, Jörg Schäfer, Gérard Blanc, Alexandra Coynel, Cécile Bossy, Magalie Baudrimont, Corine Glé, Aurélie Larrose, Sophie Renault, Emilie Strady

Silver behaviour along the salinity gradient of the Gironde Estuary

Laurent Lanceleur &Jörg Schäfer &Gérard Blanc &
Alexandra Coynel &Cécile Bossy &Magalie
Baudrimont &Corine Glé &Aurélie Larrose &Sophie
Renault &Emilie Strady

Abstract Dissolved and particulate Ag concentrations (Ag_D and Ag_P, respectively) were measured in surface water and suspended particulate matter (SPM) along the salinity gradient of the Gironde Estuary, South West France, during three cruises (2008–2009) covering contrasting hydrological conditions, i.e. two cruises during intermediate and one during high freshwater discharge (~740 and ~2,300 m^3/s). Silver distribution reflected non-conservative behaviour with 60–70 % of Ag_P in freshwater particles being desorbed by chlorocomplexation. The amount of Ag_P desorbed was similar to the so-called reactive, potentially bioavailable Ag_P fraction (60±4 %) extracted from river SPM by 1 M HCl. Both Ag_P (0.22 ±0.05 mg/kg) and Ag_P/Th_P (0.025–0.028) in the residual fraction of fluvial and estuarine SPM were similar to those in SPM from the estuary mouth and in coastal sediments from the shelf off the Gironde Estuary, indicating that chlorocomplexation desorbs the reactive Ag_P. The data show that desorption of reactive Ag_P mainly occurs inside the estuary during low and intermediate discharge, whereas expulsion of partially Ag_P-depleted SPM (Ag_P/Th_P ~0.040) during the flood implies ongoing desorption in the coastal ocean, e.g. in the nearby oyster production areas (Marennes-Oléron Bay). The highest Ag_D levels (6–8 ng/ L) occurred in the mid-salinity range (15–20) of the Gironde Estuary and were decoupled from freshwater discharge. In the maximum turbidity zone, Ag_D were at minimum, showing that high SPM concentrations (a) induce Ag_D adsorption in estuarine freshwater and (b) counterbalance Ag_P desorption in the low salinity range (1–3). Accordingly, Ag behaviour in turbid estuaries appears to be controlled by the

L. Lanceleur (*) ⦂ J. Schäfer ⦂ G. Blanc ⦂ A. Coynel ⦂ C. Bossy ⦂

M. Baudrimont ⦂ C. Glé ⦂ A. Larrose ⦂ S. Renault ⦂ E. Strady
University of Bordeaux, EPOC, UMR 5805,
33405 Talence CEDEX, France
e-mail: l.lanceleur@epoc.u-bordeaux1.fr

balance between salinity and SPM levels. The first estimates of daily Ag_D net fluxes for the Gironde Estuary (Boyle's method) showed relatively stable theoretical Ag_D at zero salinity (Ag_D^0 0 25–30 ng/L) for the contrasting hydrological situations. Accordingly, Ag_D net fluxes were very similar for the situations with intermediate discharge (1.7 and 1.6 g/day) and clearly higher during the flood (5.0 g/day) despite incomplete desorption. Applying Ag_D^0 to the annual freshwater inputs provided an annual net Ag_D flux (0.64–0.89 t/year in 2008 and 0.56–0.77 t/year in 2009) that was 12–50 times greater than the Ag_D gross flux. This estimate was consistent with net Ag_D flux estimates obtained from gross Ag_P flux considering 60 % desorption in the estuarine salinity gradient.

Introduction

The ionic form of Ag has been shown to be the most toxic Ag species (Eisler 1996; Ratte 1999), its occurrence in saltwater is almost nil and Ag chlorocomplex is the dominant dissolved Ag (Ag_D) form in saltwater (Barriada et al. 2007). However, estuarine bivalves and crustaceans accumulate Ag principally from water (e.g. Eisler 1996). The bioavailability of Ag chloride complex is mainly due to the ability of the neutral $AgCl_{(aq)}$ specie to diffuse passively through cell membrane (Engel et al. 1981). Even if $AgCl_{(aq)}$ is less toxic than the ionic form Ag^+, Ag is one of the most toxic metal for the early life stages of invertebrates and algae in marine and estuarine environments (Bryan and Langston 1992). Sublethal effects of Ag on invertebrates such as diminishing their reproductive capability have been shown in estuarine saltwater (Hornberger et al. 2000) at relatively

moderate levels of environmental contamination compared to guideline values recommended by the United States Environmental Protection Agency for Ag protection (1,920 and 3,200 ng/L in saltwater and freshwater, respectively; U.S. EPA 2002).

In former times, anthropogenic Ag inputs into aquatic systems were mainly due to acid mine drainage and metallurgy (e.g. Ayrault et al. 2010; Lanceleur et al. 2011a, b; Tappin et al. 2010). However, since the late nineteenth century, Ag use has diversified (e.g. photography, electronics; e.g. Flegal et al. 2007) and intensified, making Ag a classical tracer of urban wastewater inputs (Rozan and Hunter 2001; Sañudo-Wilhelmy and Flegal 1992; Tappin et al. 2010).

Although there is a general lack of data on dissolved Ag concentrations and fluxes in fluvial and estuarine systems at the global scale (Gobeil et al. 2005; Lanceleur et al. 2011a; Zhang et al. 2008), Ag behaviour and fate have been thoroughly studied in a few heavily polluted systems, such as the San Francisco Bay, named the 'Silver Estuary' (e.g. Flegal et al. 2007). This long-term case study has shown that the closure of a large photograph processing plant, growing Ag recycling and rehabilitation of the sewage treatment plant has decreased Ag levels in biota, sediment and water of the bay (e.g. Flegal et al. 2007; Hornberger et al. 2000).

In freshwater systems, Ag_D inputs are efficiently and rapidly (within some minutes) adsorbed onto suspended particles (Davis 1977; Smith and Flegal 1993), i.e. Ag transport and distribution closely depend on particle mobility. Consequently, sediments may stock Ag, indicating former pollution and act as both sinks and secondary sources when remobilisation occurs due to natural (floods, diagenetic recycling) or anthropogenic (dredging, dam management) processes (Audry et al. 2004; Ayrault et al. 2010; Coynel et al. 2007; Lanceleur et al. 2011b). In the Gironde watershed, 96 % of the fluvial Ag transport occurs in the particulate phase (Lanceleur et al. 2011a). When particles reach the saline part of the estuary, dissolved chlorides induce partial particulate Ag (Ag_P) desorption by the formation of dissolved Ag chlorocomplex (Luoma et al. 1995). The dissolved form of Ag being the most bioavailable (Engel et al. 1981), such desorption increases exposure and *in fine* vulnerability of estuarine and costal organisms.

The potentially bioavailable particulate Ag, estimated as the HCl-extractable fraction (Ag_{HCl}; e.g. Morse and Luther 1999) in estuarine sediment of the San Francisco Bay, was correlated with Ag concentrations in clams (*Scrobicularia plana*; Luoma et al. 1995). Furthermore, the presence of chlorides limits Ag adsorption onto solid phases, such as iron oxides (Davis 1977), probably increasing the persistence of Ag_D in saline estuarine waters. Data on Ag levels and partitioning in estuarine salinity gradients exist for a few

estuaries that are not considered turbid (e.g. Flegal et al. 2007; Tappin et al. 2010).

The Gironde Estuary (Fig. 1) is a highly turbid estuary affected by historical metal pollution (Cd, Pb, Zn, Cu, Hg, As) mainly due to geology, former mining and ore treatment (Audry et al. 2004; Castelle et al. 2007) and by agricultural activities (Masson et al. 2006). In 2004–2005, the French Mussel Watch Programme (RNO) revealed anomalously high Ag concentrations in oysters (*Crassostrea gigas*) from the estuary mouth (Chiffoleau et al. 2005). Historical records of Ag levels in reservoir sediments and in oysters from the estuary mouth suggested that (a) the former ore treatment in the watershed was a major Ag source to the Gironde Estuary for at least 50 years and (b) increasing Ag levels in oysters since the 1990s are due to more contemporary sources, likely urban wastewater (e.g. from the Bordeaux agglomeration; Fig. 1; Lanceleur et al. 2011b).

The present work aims to study dissolved and particulate Ag levels and partitioning in the salinity and turbidity gradients of the Gironde Estuary under contrasting hydrological situations, providing the first information on Ag behaviour in turbid estuaries. Furthermore, we estimate daily Ag_D net fluxes exported to the Atlantic coastal waters and discuss the potential transfer of dissolved and particulate Ag to the near oyster production zone in the Marennes-Oléron Bay.

Materials and methods

Study area

The Gironde Estuary (~170 km length; Fig. 1) is the largest estuary of the European Atlantic Coast draining a watershed (80,000 km²) with only two big urban agglomerations (Bordeaux and Toulouse; 2.7 million inhabitants).

Systematic research on its physical, geochemical and hydrological characteristics over several decades has made the Gironde Estuary a model system for the understanding of meso- to macrotidal, turbid estuaries (e.g. Audry et al. 2006; Sottolichio and Castaing 1999). Its mean annual freshwater discharge is ~1,000 m³/s over the last 90 years, but discharges tend to decrease continuously and a mean of ~770 m³/s is more representative of freshwater discharge on the last 10 years (Port Autonome de Bordeaux; DIrection Régionale de l'ENvironement). Ocean water fluxes at the estuary mouth are 30–40 times higher than fluvial inputs, and the asymmetrical progression of the tidal wave toward the upstream estuary induces a pronounced maximum turbidity zone (MTZ), where concentrations of suspended particulate matter (SPM) exceed 1 g/L in surface water and several hundreds of grams per litre in bottomwater (Sottolichio and Castaing 1999). The MTZ is typically

Fig. 1 Map of the Gironde Estuary, South West France. Kilometric point (KP): distance (kilometre) from Bordeaux. The core in the West Gironde Mud Patch (WGMP; *grey dashed area*) is described in Schmidt et al. (2005)

located in the low salinity (*S*) region and migrates up and down estuary as a function of both tidal currents and seasonal river flow variations (Sottolichio and Castaing 1999). Typical water and particle residence times were estimated at ~20−90 days and ~1−2 years respectively, depending on the season (Jouanneau and Latouche 1981).

Sampling

Particle and water samples were continuously sampled for one and a half days during three cruises, in April 2008, March and June 2009, along longitudinal profiles in the salinity and turbidity gradients in surface water (~1 m depth) of the Gironde Estuary covering contrasting hydrological situations (Table 1). All the labware in contact with the samples were acid-washed (72 h in 10 %*v/v* HNO$_3$, 14 M, J.T. Baker) and thoroughly rinsed with double deionised water (Milli-Q, Millipore). Sampling of surface waters (1 m depth) in the estuarine salinity gradient was performed with an acid-washed Niskin bottle, thoroughly rinsed with estuarine water from the site. Collected waters were immediately filtered through cellulose acetate syringe filters (0.2 μm, Sartorius) and transferred into two 60 mL acid-washed polypropylene (PP) bottles. One of the replicates was immediately UV-irradiated by passing through a quartz coil (5 m long; internal diameter 2 mm) around a UV lamp (254 nm, 40 W) at 0.5 mL/min speed (i.e. 30 min irradiation time) in order to break down dissolved/colloidal Ag metal−organic complexes (e.g. Wu et al. 2004). Following acidification (ultrapure HCl; 0.5 % *v/v*, J.T. Baker), the samples were double-bagged and sealed in polyethylene bags, then stored in the dark at 4 °C until analysis.

Suspended particles were collected by pumping 40−200 L of water (depending on the turbidity) through polyethylene tubing with a peristaltic pump (50 L/min), collected in a container previously rinsed with water from the site and immediately centrifuged (Westfalia Separator; 12,000× *g*; 60 L/h) as described elsewhere (e.g. Masson et al. 2006; Schäfer and Blanc 2002). Particle samples were stored in the dark at −20 °C in double plastic bags until arrival in the laboratory, then centrifuged at 4−6 °C to remove remaining saltwater (Jouan CR4.12; 4,000 × *g*). Fifteen additional

Table 1 Sampling station data for salinity (*S*), locations (KP; i.e. distance from Bordeaux in kilometre), suspended particulate matter (SPM), dissolved and particulate organic matter (DOM and POM), chlorophyll-*a* (Chl-*a*), particulate Ag (Ag_P), particulate Th (Th_P), Ag_P/Th_P, dissolved Ag (Ag_D) and dissolved Ag after photo-oxidation (UV-Ag_D)

Station	*S*	PK	SPM (mg/L)	DOC (mg/L)	POC (%)	Chl-*a* (μg/L)	Ag_P (mg/kg)	Th_P (mg/kg)	Ag_P/Th_P	Ag_D (ng/L)	UV-Ag_D (ng/L)
April 2008; discharge02,320 m³/s											
GMC 601	0	3	41	2.3			0.60	12.12	0.049	2.4	3.0
GMC 602	1.1	59	550	1.5	1.8		0.56	9.43	0.060	1.3	2.5
GMC 603	2.5	71	2,660	3.1	1.4		0.62	12.85	0.048	1.4	1.4
GMC 604	4.0	77	1,040	2.2	1.6		0.61	10.16	0.060	2.2	2.3
GMC 605	7.0	81	668	1.4	1.7		0.60	11.34	0.053	3.2	3.2
GMC 609	8.5	81	145	1.5	1.5		0.54	8.41	0.064	4.0	4.2
GMC 608	10.8	86	166	1.9	1.4		0.55	9.02	0.061	4.8	6.1
GMC 607	13.0	91	122	1.4	1.5		0.55	10.96	0.050	5.5	6.4
GMC 606	14.7	95	177	1.5	1.5		0.55	9.07	0.060	6.5	7.7
GMC 610	16.2	92	43	1.5	1.4		0.49	11.51	0.042		
GMC 611	20.2	95	47	1.2	1.5		0.43	10.05	0.043	6.3	7.6
GMC 612	22.3	105	30	0.8	1.4		0.32	8.35	0.038		
GMC 613	27.1	110	72	1.6	1.4		0.37	9.67	0.038	4.4	5.9
GMC 615	29.7	128	12	1.6	1.3		0.21	5.45	0.039		
GMC 614	29.8	112	32	1.8	1.2		0.28	7.00	0.040		
March 2009; discharge0747 m³/s											
METOGIR2 st11	0	2	41				0.48	11.70	0.041	1.2	1.3
METOGIR2 st10	0.1	22	256			0.4	0.34	11.97	0.029	0.8	0.9
METOGIR2 st9	0.7	30	250			0.2	0.32	10.74	0.030	0.7	0.7
METOGIR2 st8	3.4	44	198			0.5	0.36	9.00	0.040	0.9	1.0
METOGIR2 st7	6.1	55	102			1.1	0.38	12.34	0.031	1.5	1.9
METOGIR2 st6	8.4	57	63			1.1	0.35	11.00	0.032	2.1	2.7
METOGIR2 st2	11.0	87	34			0.5	0.33	12.19	0.027	1.2	2.3
METOGIR2 st5	11.2	80	38			0.6	0.32	10.62	0.030	2.2	2.3
METOGIR2 st3	13.7	89	30			0.6	0.30	12.45	0.024	2.5	2.6
METOGIR2 st4	15.6	92	27			0.5	0.28	10.10	0.028	3.2	3.2
METOGIR2 st1	17.3	87	32			0.7	0.32	11.19	0.029	4.6	4.8
VTR5 Coubre st10	18.2	95	71		1.4	0.8	0.31	11.38	0.027	4.6	5.0
VTR5 Coubre St9	19.8	103	52		1.5	0.8	0.29	12.53	0.023	5.8	6.3
VTR5 Coubre St8	23.0	108	45		1.6	0.9	0.31	12.84	0.024	3.3	5.2
VTR5 Coubre St7	25.4	112	31		1.5	1.2	0.25	12.14	0.021	3.9	4.3
VTR5 Coubre St6	26.8	113	40		1.6	1.4	0.27	12.21	0.022		4.3
VTR5 Coubre St5	27.7	115	35		1.6	1.4	0.25	12.20	0.021		4.5
VTR5 Coubre St4	29.0	118	31		1.7	1.2	0.23	11.93	0.019	4.6	4.5
VTR5 Coubre St2	29.9	129	21		1.9	0.8	0.24	12.25	0.020	4.2	4.3
VTR5 Coubre St3	30.7	123	28		1.7	1.4	0.22	13.00	0.017		3.8
VTR5 Coubre St1	32.3	135	12		6.3	2.3	0.21	8.40	0.025		1.8
June 2009; discharge0729 m³/s											
VTR6 Coubre 10	24.6	94	15		2.4	1.7	0.29	10.92	0.026	2.9	6.5
VTR6 Coubre 9	24.8	103	11		3.2	1.9	0.33	11.69	0.028	4.0	8.0
VTR6 Coubre 8	26.7	108	9			2.0	0.29	11.46	0.025	2.6	6.5
VTR6 Coubre 7	27.9	112	5		4.2	0.5	0.27	10.54	0.026	2.0	6.0
VTR6 Coubre 5	28.0	115	10		3.1	1.4	0.30	12.17	0.025	3.7	6.1
VTR6 Coubre 6	29.4	114	9		3.6	1.9	0.23	10.09	0.023	2.5	4.3
VTR6 Coubre 3	29.5	124	7		6.8	1.7	0.23	9.33	0.024	2.4	3.4

Table 1 (continued)

Station	S	PK	SPM (mg/L)	DOC (mg/L)	POC (%)	Chl-a (µg/L)	Ag_P (mg/kg)	Th_P (mg/kg)	Ag_P/Th_P	Ag_D (ng/L)	UV-Ag_D (ng/L)
VTR6 Coubre 4	30.1	120	7		3.5	2.0	0.18	5.05	0.036	2.4	3.3
VTR6 Coubre 1	31.1	133	9		8.4	1.9	0.20	7.95	0.026	2.3	3.0
VTR6 Coubre 2	31.1	129	7		5.5	1.5	0.23	8.11	0.028	2.4	2.7
WGMP							0.26	9.6	0.027		

Mean results (n03) for the West Gironde Mud Patch (WGMP) represent the pre-industrial period (1926–1940) for the Gironde watershed

freshwater SPM samples were collected twice monthly at Bordeaux (Fig. 1; Table 2) between March and October 2008. Sample location was defined by the distance from Bordeaux in kilometre, Bordeaux representing the kilometric point zero (KP0; Table 1). All SPM samples were dried at 50 °C, then powdered and homogenised with an agate mortar and stored in sealed double PE bags in the dark.

Suspended particulate matter, particulate and dissolved organic carbon and chlorophyll-a measurements

SPM concentrations in surface water were determined by filtration of precise water volumes through dry, pre-weighed filters (Whatman GF/F, 0.7 µm). The filters were then dried to constant weight at 45 °C and re-weighed.

Particulate organic carbon (POC) was measured directly from the dry, powdered and homogenised estuarine material using a carbon/sulphur analyser (LECO, CS-125). Prior to their combustion in an induction furnace, samples were acidified in crucibles with 2 M HCl to remove carbonates, then dried at 60 °C to remove inorganic C and most of the remaining acid and water (e.g. Abril et al. 2002). The quality control included measurement of certified reference materials (e.g. LECO 501–503). Accuracy was within 5 % of the certified values and the analytical error (RSD) generally better than 5 %. The analysis of dissolved organic carbon (DOC) in samples of filtered estuarine water (GFF filter, combusted at 450 °C during 5 h) was performed by the high temperature catalytic oxidation method using a total organic carbon (TOC) analyser (Shimadzu, TOC 5000) as described elsewhere (Lemaire et al. 2006). Detection limits (3 sigma of the blank values) varied from 0.3 to 0.4 mg/L and reproducibility was generally better than 5 % (RSD). Calibration was performed by dilution of a potassium phthalate solution. Details on the applied method and its analytical quality evaluated in an intercalibration between four European laboratories are given elsewhere (Abril et al. 2002).

Chlorophyll-a (Chl-a) concentrations were measured during the 2009 cruises. Water was collected and immediately filtered through GFF Whatman filters (25 mm) and stored at −80 °C until their analysis by fluorometry (Trilogy, Turner). Acetone (90 %) was used as extraction solvent (Holm-Hansen et al. 1965). Dilutions of a Chl-a standard solution (Anacystis nidulans, 1 mg/L; C-6144; Sigma-Aldrich) were used to calibrate the fluorometer.

Particulate silver (Ag_P) analyses

For total Ag_P concentration analyses, SPM was homogenised and 30 mg subsamples were digested in acid-washed PP tubes (DigiTUBEs®, SCP Science) using 1.5 mL HCl (12 M, Plasmapur, SCP Science), 0.75 mL HNO_3 (14 M, Plasmapur, SCP Science) and 2 mL HF (26 M, Plasmapur, SCP Science). The reactors were then heated at 110 °C for 2 h in a heating block (DigiPREP MS®, SCP Science). After cooling, the digestates were evaporated to dryness. Each sample was brought to 10 mL using 150 µL HNO_3 (14 M, Plasmapur) and Milli-Q water (Larrose et al. 2010).

The acid-soluble Ag_{HCl} fraction, also called the reactive fraction (i.e. 1 M HCl extractible; e.g. Morse and Luther 1999), was extracted from freshwater SPM collected at Bordeaux (Table 2) by mixing subsamples (200 mg) with 12.5 mL of 1 M HCl (Plasmapur, SCP Science) for 24 h using end-over-end tumbling at 12 rpm. After centrifugation (3,000 rpm; 20 min) the supernatant was retrieved and evaporated to dryness and the residues were brought to 10 mL as described for the tri-acid digestion procedure (see above). Single extractions by 1 M HCl were designed to extract trace metals bound to the reactive phases (e.g. Morse and Luther 1999) and have been proposed as a proxy to estimate the potentially bioavailable metal fractions, i.e. the fractions which may represent a threat to aquatic biota (Bryan and Langston 1992; Langston et al. 1999).

Both the solutions containing the total (Ag_P) and the HCl-extracted Ag_{HCl} fractions were analysed by quadrupole ICP-MS (X7, Thermo-Fisher). As part of the quality control, the analytical accuracy was checked by parallel analyses of the international certified reference sediment NCS-DC-70317 (n 06). The Ag recovery was evaluated at 112±5 % and precision (RSD) was better than 4 % at the 0.32 mg/kg level. Detection limits for total Ag_P estimated as three times the standard deviation of method blanks obtained for the

Table 2 Sampling date data for suspended particulate matter (SPM) collected at Bordeaux between March and October 2008, particulate Ag (Ag_P), particulate Th (Th_P), Ag_P/Th_P, percentage of Ag_P (Ag_{HCl}) and Th_P (Th_{HCl}) extracted by 1 M HCl from SPM and resulting residual Ag (Ag_R)

Date	SPM (mg/L)	Ag_P (mg/kg)	Th_P (mg/kg)	Ag_P/Th_P	Ag_{HCl} (%)	Th_{HCl} (%)	Ag_R (mg/kg)
03 March 2008	427	0.46	11.3	0.040	64	2	0.16
17 March 2008	341	0.49	14.7	0.033	56	2	0.21
01 April 2004	59	0.47	11.0	0.043	62	2	0.18
14 April 2008	54	0.46	14.0	0.033	55	1	0.21
28 April 2008	41	0.87	13.6	0.064	61	1	0.34
13 May 2008	33	0.78	9.2	0.084	70	2	0.24
02 June 2008	230	0.50	10.3	0.049	58	1	0.21
16 June 2008	142	0.38	10.4	0.036	57	1	0.16
03 July 2008	125	0.65	8.8	0.073	61	1	0.25
21 July 2008	892	0.46	10.6	0.043	57	3	0.20
31 July 2008	1,230	0.47	11.2	0.042	58	2	0.20
28 August 2008	1,026	0.40	11.2	0.036	56	3	0.18
18 September 2008	3,027	0.43	15.0	0.029	60	2	0.17
29 September 2008	5,232	0.40	14.2	0.028	59	2	0.17
16 October 2008	4,642	0.47	15.3	0.031	49	2	0.24

total digestion procedure were 0.001 mg/kg (n 06). In order to remove the grain size effect (Larrose et al. 2010; Van Calsteren and Thomas 2006), the measured Ag_P was normalised against particulate Th concentrations (Th_P; Tables 1 and 2) obtained for the same samples.

Dissolved silver (Ag_D) analyses

The dissolved Ag concentrations of filtered sample (Ag_D) and UV-irradiated replicates (UV-Ag_D) were measured by ICP-MS after on-line solid−liquid ion exchange (preconcentration and matrix separation) using isotope dilution (Barriada et al. 2003; Ndung'u et al. 2006; Yang and Sturgeon 2002). Briefly, 12 mL samples were spiked 24 h before analysis with a known amount of ^{107}Ag in solution (Oak Ridge National Laboratory, TN, USA). After this equilibration time, the 12 mL samples passed through a minicolumn (85 μL internal volume; Global FIA, USA) filled with a strong anion-exchange resin (Dowex 1-X8, 200−400 mesh, Supelco) to retain the Ag_D species (negatively charged Ag chlorocomplexes represent 85 % of Ag_D species present at only 50 mM chloride concentration; Barriada et al. 2007). The saline matrix was rinsed off with Milli-Q water, followed by on-line elution (HNO$_3$, 2 M, Plasmapur, SCP Science) to transport the preconcentrated Ag_D species to the ICP-MS. The peak areas of the transient signals recorded were integrated with PlasmaLab software (Thermo Scientific). From the resulting modified isotope ratios, Ag_D concentrations were calculated using the following equation (Rodriguez Martin-Doimeadios et al. 2003):

$$C_x = C_y \times \frac{m_y}{m_x} \times \frac{A_y - B_y \times R_n}{B_x \times R_n - A_x} \times \frac{AW_x}{AW_y}$$

where C_x is the analyte concentration (nanogram per millilitre); C_y is the concentration of spike (nanogram per millilitre); m_y is the volume of spike used to prepare the blend solution of sample and spike (millilitre); m_x is the volume of the sample used (millilitre); A_y is the abundance of the reference isotope in the spike; B_y is the abundance of the spike isotope in the spike; A_x is the abundance of the reference isotope in the sample; B_x is the abundance of the spike isotope in the sample; R_n is the measured reference/spike isotope ratio (mass bias-corrected) in the spiked sample; AW_x is the atomic weight of analyte in the sample and AW_y is the atomic weight of the spike.

Accuracy and precision were evaluated from parallel analyses of international certified reference freshwater (NIST-1640), estuarine water (SLEW-3) and nearshore seawater (CASS-4; Table 3). Only NIST-1640 is certified for Ag and SLEW-3 has an informational value of 3 ng/L. However, values obtained for SLEW-3 and CASS-4 (with or without UV treatment) were comparable to Ag concentrations reported by Morford et al. (2008), Ndung'u et al. (2001, 2006) and Yang and Sturgeon (2002). Interestingly, dissolved Ag levels obtained for CASS-4 tended to be higher after UV treatment (Table 3), which is supported by the data from Ndung'u et al. (2006). Accuracy obtained for the analyses of NIST-1640 diluted 1,000-fold (n03) was 96± 5 % and precision (RSD) was better than 2 % at the 0.8 ng/L level (Table 3). The detection limit (3 SD of 12 mL sample blanks) was 0.17 ng/L without UV treatment (n 04) and 0.28 ng/L with UV treatment (n04). Comparison of data was done using the Spearman rank correlation coefficient (R), a non-parametric method, considered significant when the p value is inferior to 5 %.

Table 3 Mean±standard deviation of dissolved Ag (Ag$_D$) concentrations in estuarine and nearshore seawater certified reference material (SLEW-3, CASS-4, CASS-5) and freshwater standard reference material (NIST-1640)

Certified reference waters	Salinity	Certified Ag$_D$ (ng/l)	Measured Ag$_D$ (ng/l)	Number of individual analyses	Reference
Without UV treatment					
NIST-1640 (diluted 1,000-fold)	0	7.62	7.49±0.10	3	This study
CASS-4	30.7	nd	6.53±0.45	3	This study
			5.72±0.32	5	Morford et al. (2008)
			6.36±1.08	2	Morford et al. (2008)
			5.72±0.32	15	Morford et al. (2008)
			5.42±0.08	3	Yang and Sturgeon (2002)
			6.11±0.90	7	Ndung'u et al. (2001)
CASS-5	33.5	nd	1.74±0.04	5	This study
With UV treatment					
NIST-1640 (diluted 1,000-fold)	0	7.62	7.21±0.54	3	This study
SLEW-3	15	~3	2.64±0.39	3	This study
			2.97±0.77	33	Ndung'u et al. (2006)
CASS-4	30.7	nd	10.19±0.86	3	This study
			8.48±1.96	21	Ndung'u et al. (2006)

Daily Ag$_D$ net flux estimation

The commonly applied method for estimating dissolved metal net fluxes from estuaries to the coastal ocean (Boyle et al. 1974) is based on the dissolved element distribution in the estuarine high salinity range. According to Boyle et al. (1974, 1982), the instant net fluxes (F_t) of a dissolved element X across an isohaline S at time t is:

$$F_t = Q_t \left[[X] - [S] \frac{d[X]}{d[S]} \right]$$

where Q_t is the freshwater discharge at time t, $[X]$ is the concentration of the element of interest and $[S]$ is salinity. If the relation between the dissolved element concentration and the salinity is linear (conservative behaviour), $d[X]/d[S]$ is constant and equal to the slope of the segment representing this relation in the concentration–salinity diagram. In this case, for any salinity $[S]$ belonging to the linearity range, $[X]_S - [S] \times (d[X]_S/d[S])$ is constant and equal to the intercept $[X]^0$ of the straight line extrapo- lated from this segment. Accordingly, the net instanta- neous flux of the element through any isohaline in the linearity range is:

$$F_t = Q_t [X]^0$$

Using the average daily freshwater discharge Q_{fw} pro- vides an estimate of the daily net flux (F_{NET}) as follows:

$$F_{NET} = Q_{fw} [X]^0$$

The 'Port Autonome de Bordeaux' and the 'DIrection Régionale de l'ENvironement' provided the freshwater dis- charge data for the Garonne and the Dordogne Rivers, the two main tributaries of the Gironde Estuary (Fig. 1). Discharge data for the Gironde Estuary were estimated from the sum of the Garonne and the Dordogne River discharges added 15 % to consider the commonly neglected contributions of minor tributaries to the Gironde Estuary, such as the Isle River and several small tributaries downstream of the discharge mea- surement stations (Schäfer et al. 2002).

Results

Hydrological conditions

The first cruise in April 2008 covered a flood event (mean freshwater discharge 2,320 m^3/s), causing a strong salinity front at the seaward end of the estuary with a 1–30 salinity gradient between KP60 and KP130 (Fig. 1). The March and June 2009 cruises took place in intermediate discharge con- ditions with mean freshwater flow rates of 747 and 729 m^3/ s, respectively. June cruise focussed on Ag behaviour in the seaward end of the estuarine salinity gradient ($S > 25$), where SPM concentrations were generally low (Table 1). Annual freshwater fluxes to the Gironde Estuary for years 2008 (30.5 km^3) and 2009 (26.7 km^3) were typical of the 1990– 2007 period (18–50km^3/year, mean 27±7 km^3/year; Dabrin et al. 2009; Schäfer et al. 2002).

SPM, DOC, POC and Chl-*a* along the estuarine salinity gradient

The SPM concentrations in surface water during the flood situation (April 2008) ranged from 12 to 2,660 mg/L, i.e. showed values commonly observed in this turbid estuary (Dabrin et al. 2009), with a well-developed MTZ in the 1−7 salinity range (between KP70 and KP80; Table 1). During the moderate discharge situation in March 2009, the highest SPM concentrations of the MTZ were also located in the low salinity range ($0.1 < S < 0.7$) but upstream from its position in the previous flood event of April 2008 (KP2 to KP55; Table 1). The SPM concentrations sampled were not greater than 256 mg/L but higher concentrations occurred between KP2 and KP22 that were not sampled. The SPM concentrations at Bordeaux ranged from 0.03 to 5.23 g/L between March and October 2008 (Table 2). The highest concentrations (>1 g/L) were reached in low discharge period (August to October) when the mean Gironde discharge was 223 ± 54 m^3/s.

In April 2008, DOC ranged from 0.8 to 3.1 mg/L with the highest value coinciding with maximum SPM, i.e. in the low salinity range (Table 1). Level of POC in the Gironde Estuary (KP < 100; 1.5 ± 0.2 %; Table 1) was equal to the value given by Etcheber et al. (2007). Higher POC level (up to 6.3 %) occurred at the seaward end (KP > 100) probably due to marine primary production.

During the low turbidity spring period (March 2009), Chl-*a* concentrations ranged from 0.2 to 2.3 µg/L from salinity 0.1 to 32 (Table 1) and increased significantly with salinity (R 0.60, $p<0.05$, n 020). Similar Chl-*a* values (0.5−2.0 µg/L) occurred in the high salinity range (S 025−31) in June 2009, but were not related with salinity (R 0.10, $p>0.05$, n 010). Such relatively low Chl-*a* levels are typical for this turbid estuary and reflect the very limited light penetration and photochemical processes in the water column (Irigoien and Castel 1997).

Particulate silver distribution along the salinity gradient

Particulate Ag concentrations in Bordeaux freshwaters were 0.6 and ~0.5 mg/kg in April 2008 and in March 2009, respectively (Fig. 2). These values are similar to typical Ag_P concentrations measured in the Garonne River during the preceding decade (Lanceleur et al. 2011a). As salinity increased Ag_P decreased progressively to ~0.2 mg/kg in coastal seawater ($S > 30$), whatever the hydrological situation. A slightly different distribution was observed when Ag_P concentrations were normalised by total particulate thorium (Th_P; Table 1). In the freshwater zone, Ag_P/Th_P ratios were relatively similar in April 2008 and March 2009 (0.049 and 0.041, respectively), i.e. independent from hydrological conditions. However, in the marine estuary ($S>25$), Ag_P/Th_P was clearly

lower during moderate discharge (means of 0.021 and 0.027, respectively for March and June 2009; Table 1) than during the flood (0.039; April 2008), when Ag_P/Th_P was close to typical freshwater values.

The SPM samples periodically recovered at Bordeaux tended to show two distinct Ag_P levels, depending on SPM concentrations (Table 2). From March to July 2008 (SPM < 1 g/L; n 010), mean Ag_P concentration was 0.55 ± 0.16 mg/kg (Ag_P/Th_P 0 0.050 ± 0.018), of which 60 ± 4 % were extracted by 1 M HCl. Accordingly, the Ag concentration in the residual fraction (Ag_R; not extracted by 1 M HCl) was 0.22 ± 0.05 mg/kg (Ag_R/Th_P 0 0.020 ± 0.005). During the presence of the MTZ at Bordeaux (August to October 2008, SPM > 1 g/L; n 05), Ag_P was 0.44 ± 0.03 mg/kg (Ag_P/Th_P 0 0.033 ± 0.006) with 56 ± 5 % extracted by HCl, corresponding to a Ag_R of 0.19 ± 0.03 mg/kg (Ag_R/Th_P 0 0.015 ± 0.003). In the sediments from the West Gironde Mud Patch (n 03, data not shown; Fig. 1), Ag_P (0.26 ± 0.02 mg/kg) and Ag_R (0.23 ± 0.02 mg/kg) were similar with a common Th_P-normalised value (0.027 ± 0.001), i.e. nearly all Ag_P was in the residual fraction.

Dissolved silver distribution in the salinity and turbidity gradients

The distribution of Ag_D and UV-Ag_D along the salinity gradient followed a bell-shaped curve (Fig. 3), with UV-Ag_D from 0.7 to 8.0 ng/L and maximum values located in the 15−25 salinity range. Minimum concentrations for both Ag_D and UV-Ag_D occurred either in the low salinity range ($0 \leq S \leq 3$) where SPM concentrations were high, or in coastal seawater ($S \geq 30$) at the estuary mouth. Values of UV-Ag_D recorded in Bordeaux freshwaters were 1.2 ng/L in March 2009 and 2.4 ng/L in April 2008, whereas the respective UV-Ag_D at the seaward end were 1.8 and 4.4 ng/L (i.e. 1.4- and 2-fold greater than freshwater values).

Effect of UV treatment

The Ag_D fraction retained by the anionic chelating resin in the matrix separation step without previous UV treatment probably contains the anionic dissolved Ag complexes and 'labile' Ag metal−organic complexes. The UV irradiation prior to ion exchange chromatography aimed at breaking down (as far as possible) dissolved and colloidal (filter passing) Ag metal−organic complexes (Batley and Florence 1976), which are not retained by the anionic chelating resin without UV treatment. Accordingly, the UV-Ag_D fraction comprises both the Ag_D fraction and 'non-labile' Ag dissolved/colloidal metal−organic complexes, i.e. UV-Ag_D may be considered as approaching the total dissolved Ag concentration. The difference between UV-Ag_D and Ag_D, attributed to 'non-labile' Ag dissolved/colloidal metal−organic complexes,

Fig. 2 Particulate Ag concentrations (Ag_P) and Ag_P/Th_P for the April 2008 (a), the March 2009 (a) and the June 2009 (c) cruises along the salinity gradient
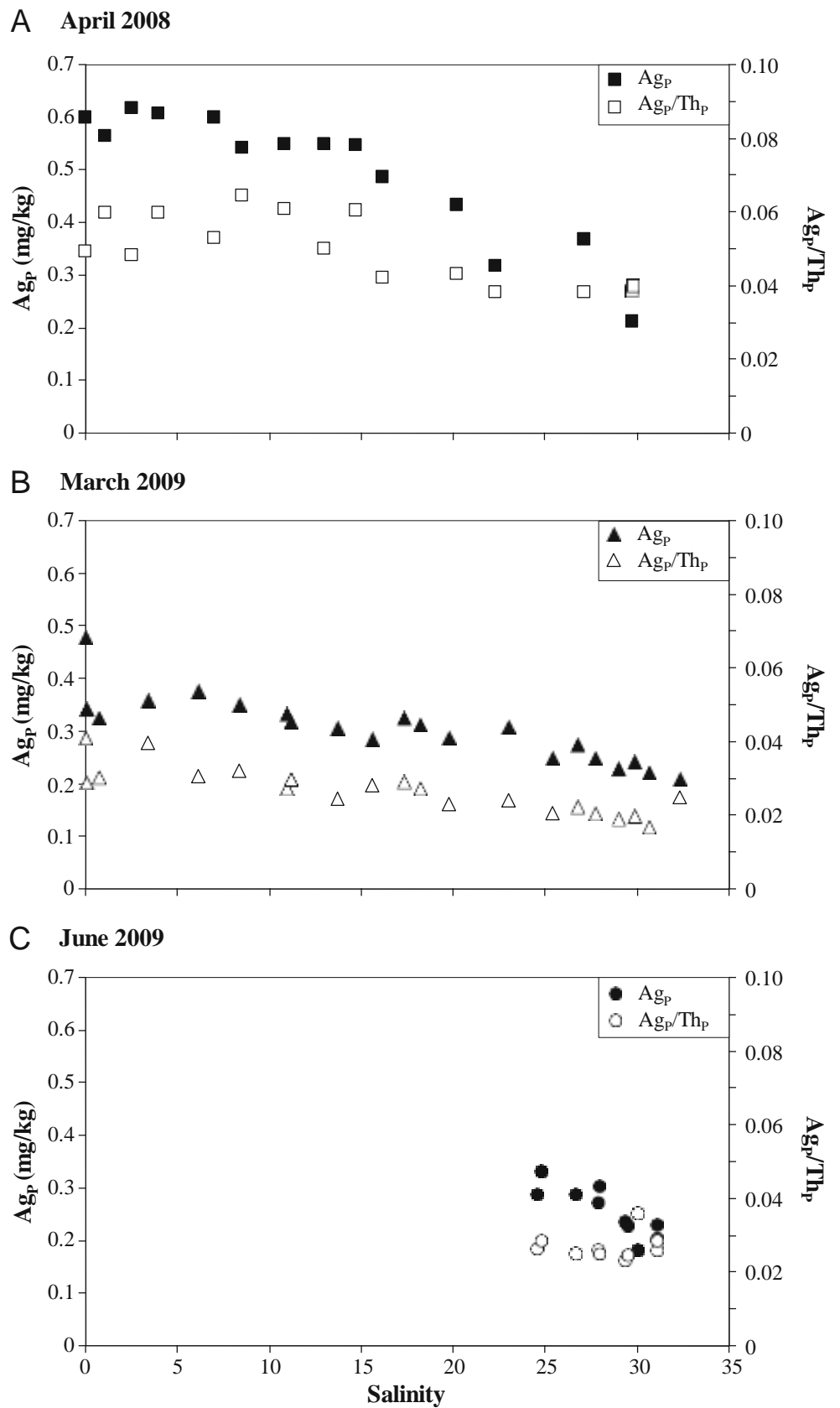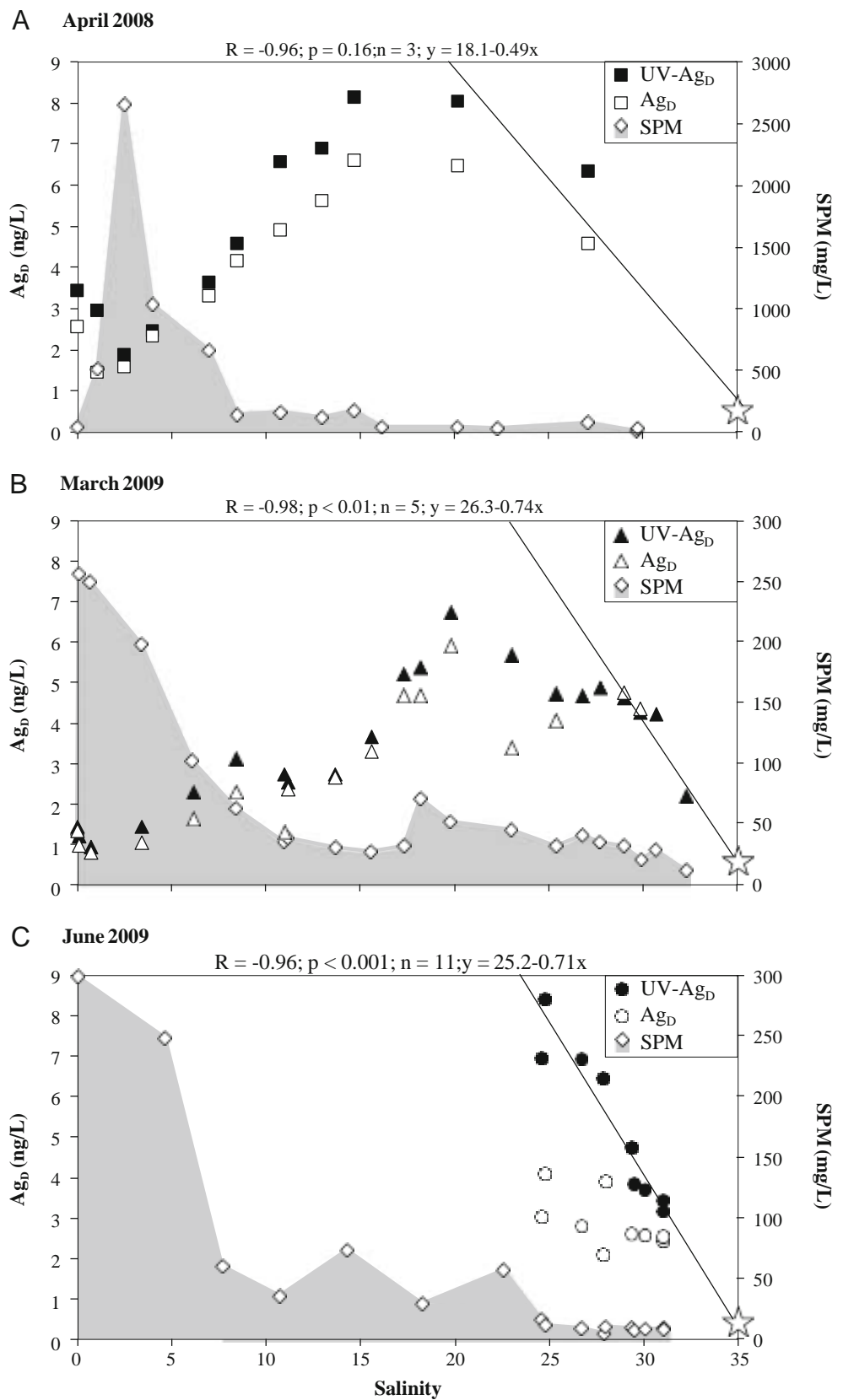
Fig. 3 Dissolved Ag concentrations (Ag_D and UV-Ag_D) and SPM for the April 2008 (a), the March 2009 (b) and the June 2009 (c) cruises along the salinity gradient. *Black line*: linear regression of used for net UV-Ag_D flux (Boyle et al. 1974, 1982) with correlation coefficient, *p* value at the 95 % confidence level, number of points used for each regression and equation of the dilution line. The *white star* represents North Atlantic Ocean Ag_D (data from Rivera-Duarte et al. 1999)

A **April 2008**

R = -0.96; p = 0.16; n = 3; y = 18.1-0.49x

B **March 2009**

R = -0.98; p < 0.01; n = 5; y = 26.3-0.74x

C **June 2009**

R = -0.96; p < 0.001; n = 11; y = 25.2-0.71x

may provide valuable information on operationally defined dissolved Ag speciation (Batley and Florence 1976).

The results obtained from the three cruises showed that UV-Ag_D may be equal to or up to 3-fold greater than Ag_D,

depending on both salinity and SPM concentration (Fig. 3). For example, in April 2008, Ag_D represented 100 % of UV-Ag_D in the MTZ (SPM 0 2,660 mg/L; S $0$2.5) and 75 % upstream from the MTZ (SPM 0 75 mg/L; S $0$27.1), i.e. the measured 'non-labile' Ag fraction accounted for 25 % in the upstream estuary. The 2009 March and June data (Fig. 3b, c) also suggest that the non-labile fraction was high (up to 67 % of UV-Ag_D) at S >20 and decreased to values ranged from close to 0 to 13 % at higher salinities (S> 29), relatively independent from SPM concentrations.

Discussion

Particulate silver behaviour in the estuary

The major part (96±2 %) of Ag provided to the Gironde Estuary by its main tributary, i.e. the Garonne River, is associated to the particulate phase (Lanceleur et al. 2011a). It is therefore important to understand the fate of Ag_P in the estuarine salinity and turbidity gradients.

The strong decrease in Ag_P along the salinity gradient of the highly turbid Gironde Estuary is consistent with that reported for Japanese rivers flowing to Tokyo Bay (Ag_P decrease from 0.1 to 0.03 mg/kg; i.e. 70 %; Zhang et al. 2008) and was attributed to desorption processes induced by chloride complexation (Ciffroy et al. 2003; Luoma et al. 1995). Comparing Ag_P in SPM from the freshwater and the marine endmembers in April 2008 and March 2009 clearly suggests that 60 to 67 % of Ag_P was desorbed, i.e. added to the dissolved phase along the salinity gradient (Fig. 2a, b). This fraction mobilised is equivalent to Ag_{HCl} in SPM from the freshwater estuary (60 ± 4 %; Bordeaux, March–July 2009, Table 2) upstream from the MTZ. Slightly lower Ag_{HCl} fractions (56 ± 5 %; Bordeaux, August–October 2009) occurred in the presence of the MTZ, probably because MTZ particles are a mix of freshwater particles and older SPM from which Ag and other metals (e.g. Cd, Cu) have previously been partly mobilised (Masson et al. 2006). The Ag_{HCl} fractions in freshwater SPM from the Gironde Estuary are greater than, but consistent with, those of oxidised surface sediment from 17 English estuaries (25–40 %; Luoma and Bryan 1981). This may be due to (a) differences in SPM origin/composition and/or (b) previous partial Ag desorption induced by chlorides. The latter hypothesis was supported by experimental study showing that 55–85 % of the particle-bound Ag in estuarine sediments previously exposed to a 80 µg/L Ag solution during 14 days was extractable by HCl (0.5 M; Luoma et al. 1995).

In a previous work, Lanceleur et al. (2011a) have established the grain size corrected geochemical background of Ag in SPM from the Gironde Estuary watershed as Ag_P/Th_P 0 0.026. Sediments constituting the West Gironde Mud Patch, localised near the North Channel of the Gironde Estuary (Fig. 1), are mainly derived from estuarine SPM (Schmidt et al. 2005). In fact, Ag_P/Th_P values (Ag_P/Th_P 0 0.027; $n$$0$3) in these sediments representing the 1926–1940 period (40 cm depth), i.e. before the increase of metalworking industry in the Lot River basin (Audry et al. 2004; Schmidt et al. 2005), are similar to those observed in SPM from the high salinity range during intermediate freshwater discharge (~0.027; March and June 2009). Conversely, the Ag_P/Th_P value (0.040) in SPM from the high salinity range (S>20) was clearly greater during high discharge and higher tidal currents (tidal coefficient$0$65) in April 2008 as a result of lower Th_P values (Table 1). These results suggest (a) that Ag desorption from SPM is highly efficient during intermediate discharge and results in residual Ag_P/Th_P levels similar or lower than the geochemical background and (b) that during the flood event, SPM from the estuary mouth were coarser, probably due to an increasing fraction of fine sand, the dominant sediment in the estuary mouth (Larrose et al. 2010), and still contained potentially desorbable Ag_P.

Based on the geochemical background, Lanceleur et al. (2011a) attributed Ag_P/Th_P ratios higher than 0.026 to the adsorption of Ag_D released by anthropogenic activities on SPM. Consequently, the anthropogenic Ag_P fraction belongs to the operationally defined reactive Ag_P fraction (i.e. 1 M HCl extractable). Because Th is highly insoluble in seawater (Van Calsteren and Thomas 2006), this means that (a) the estuarine salinity mobilises at least the equivalent of whole anthropogenic component of Ag_P (similar to 1 M HCl) and (b) this anthropogenic fraction is potentially bio-available. Assuming that the Ag desorbed in the salinity gradient is bioavailable, particulate Ag transport to the estuary and subsequent desorption is probably the major Ag source accounting for the anomalously high Ag concentrations in estuarine oysters (up to 110 mg/kg, dry weight; Lanceleur et al. 2011b). During the flood, Ag desorption inside the estuary is incomplete, probably due to the relatively short particle residence times (~1 week), and expulsion of estuarine particles to the coastal ocean is at maximum (Castaing and Allen 1981). In these conditions, Ag release from particles probably occurs in the coastal seawater and may affect the nearby Marennes Oléron Bay, where oyster cultures are exposed to particles derived from the Gironde Estuary (Strady et al. 2011).

Dissolved Ag distribution

In river water, Ag_D rapidly sorbs onto particles (Davis 1977; Smith and Flegal 1993), but this process is reversible, as Ag_P also is rapidly desorbed (e.g. by 0.5 M HCl; Luoma et al. 1995). In the brackish part of the Gironde Estuary, the Ag_D profiles are typical for metals undergoing chlorocomplexation (e.g. Cd, Dabrin et al. 2009), i.e. they show a mid-

salinity maximum in the dissolved phase, reflecting the balance between induced complexation processes and dilution by seawater (e.g. Comans and van Dijk [1988]). Accordingly, the observed increase in Ag_D concentrations with salinity (Fig. [3]) was attributed to chloride-induced desorption, which is consistent with the results from other estuaries (Luoma et al. [1995]; Tappin et al. [2010]; Wen et al. [1997]).

Although very high SPM concentrations (e.g. 2.8 g/L in April 2008) probably imply very high amounts of potentially desorbable Ag in the MTZ, no addition of Ag_D was observed in the respective salinity range ($0 < S < 3$; Fig. [3]). This suggests that in highly turbid conditions, adsorption on SPM prevails over chloride-induced desorption at low salinity. Our results obtained for the Ag partitioning in the Gironde Estuary are in good agreement with previous experiments showing that >99 % of Ag from a 100 mL solution (80 µg/L) was adsorbed by 2 g of oxidised estuarine sediment in 24 h at salinity 20 (Luoma et al. [1995]).

The seaward part of the bell-shaped curve (Fig. [3]) reflects dilution of Ag-rich estuarine waters by seawater (Ag_D 0 0.39 ng/L, station 4, North Atlantic Ocean; Rivera-Duarte et al. [1999]). This seaward-dipping Ag_D gradient follows the gradient of Ag bioaccumulation in oysters at three stations within the Gironde Estuary mouth (La Fosse site, $15 < S < 20$; Fig. [1]) towards the outer station (Bonne Anse, $S > 25$; Chiffoleau et al. [2005]; Lanceleur et al. [2011b]). The Ag_D values in the Gironde Estuary were similar in magnitude to those reported for the Fal Estuary (southwest England; 9.8 ± 6.7 ng/L; Tappin et al. [2010]) receiving acid mine drainage from numerous disused mine workings over a protracted period, the inner part of the Fal Estuary, i.e. Restronguet Creek, being considered as the most metal-polluted estuary in the UK (Tappin et al. [2010]). However, the Ag_D distributions along the salinity gradients were different between the highly turbid Gironde Estuary (SPM 5–2,660 mg/L) and the weakly turbid Fal Estuary (SPM 2–9 mg/L), where Ag_D increased from 3.5 ng/L in freshwater to a maximum of 19.5 ng/L as soon as salinity reaches 6. This suggests that Ag_D levels and distribution in estuarine salinity gradients strongly depend on the balance between desorption and adsorption, i.e. SPM levels and distribution.

Wen et al. ([1997]) showed that Ag was partially associated with colloidal macromolecular organic matter in the Trinity River Estuary (15–70 % of Ag_D species in <0.45 µm filtered water were greater than 1 kDa, decreasing with increasing salinity). In the Gironde Estuary, maximum DOC levels typically occur in the MTZ (Table [1]) reflecting (a) accelerated particulate organic matter decomposition due to oxic and anoxic oscillations in the MTZ and (b) accumulation of DOC in the fluid mud periodically resuspended by tidal currents and/or dredging (Abril et al. [1999]). However, despite high DOC levels, Ag_D and UV-Ag_D were similar in nearly all samples from the well-developed MTZ for SPM >

200 mg/L (April 2008; Fig. [3a]), suggesting the absence of non-labile filter-passing colloidal metal-organic Ag complexes in the MTZ. In contrast, at low SPM levels, the non-labile fractions accounted for up to 25 % of Ag_D and were not correlated with DOC in April 2008. Further speciation investigations combining different cut-offs and separation techniques (e.g. Lemaire et al. [2006]) are needed to better understand the behaviour of dissolved/colloidal Ag species in the Gironde Estuary.

Dissolved silver net fluxes

As water and particles in the Gironde Estuary have very different residence times (respectively 20–90 days and ~1–2 years; Jouanneau and Latouche [1981]), there is no simple relation between Ag_D and Ag_P concentrations and fluxes. However, taking the average Ag_P concentration (0.55 ± 0.16 mg/kg) in SPM from Bordeaux sampled in freshwater and at low turbidity (Table [2]), a potential desorption equal to 60 % of Ag_P and the average SPM gross flux to the estuary during the past decade ($1.5 \ 10^6$ t/year), the annual Ag_D net flux was roughly estimated at 0.35–0.64 t/year. This estimate is consistent with that obtained from Boyle's method (Boyle et al. [1974], [1982]) applied to our dataset. For this, a marine endmember (Ag_D 0 0.39 ng/L; measured at 56° N 25.5° W; Rivera-Duarte et al. [1999]) was plotted on our Ag_D profiles (Fig. [3]), and the theoretic Ag_D concentrations were estimated at zero salinity (Ag_D^0) using the UV-Ag_D data.

The Ag_D^0 values obtained for intermediate freshwater discharge conditions were 26 ± 8 ng/L in March 2009 (n0 5; R0–0.98; $p < 0.01$) and 25 ± 4 ng/L in June 2009 (n 011; r0–0.97; $p < 0.001$), stated at the 95 % confidence level. The dataset obtained for the flood (April 2008) did not allow a confidence interval estimation but the linear decrease in Ag_D in the high salinity range suggested Ag_D^0 was ~25 ng/L, i.e. similar to the other profiles. This observation is consistent with previous work on cadmium (Cd) net fluxes in the Gironde Estuary, showing that the theoretical dissolved Cd concentration at zero salinity (Cd_D^0) did not vary much during intermediate and high discharge (Dabrin et al. [2009]). The daily Ag_D net flux was estimated at 5.01 g/day during the flood (April 2008) and 1.68 ± 0.52 g/day (March 2009) and 1.57 ± 0.25 g/day (June 2009) for intermediate freshwater discharges. Applying an Ag_D^0 of 25 ± 4 ng/L (June 2009) to the annual freshwater flux in the Gironde Estuary, we estimated annual Ag_D net fluxes (i.e. ejected off the Gironde Estuary) at 0.64–0.89 t/year in 2008 and 0.56–0.77 t/year in 2009.

The estuarine Ag mass balance (i.e. input vs output) was improved by accounting the particle and water residence times in the estuary (1–2 years and 20–90 days, respectively). Accordingly, we combined the estimated Ag_P gross fluxes during 2006–2008 (data from Lanceleur et al.

2011a), the 2008/2009 Ag_D gross fluxes via the Garonne and Dordogne Rivers (Lanceleur et al. 2011a; Garonne River: La Réole site; Dordogne River, 40 % and 27 % contribution to Ag_D and Ag_P gross fluxes to the Gironde Estuary, respectively) and the Ag_P desorption potential of 60 % (this study). The resulting potential (estimated from river input) Ag_D net flux of 0.45–0.74 t/year for 2008/2009 was very close to our Ag_D net flux obtained from Boyle's method (estimated at the Gironde Estuary highest salinities), i.e. the contribution of intra-estuarine Ag sources (e.g. sorption/desorption of Ag with bed sediments and benthic fluxes of Ag_D; Rivera-Duarte and Flegal 1997) appeared small (<20 %).

However, this mass balance does not take into account potential Ag desorption in the coastal ocean from particles exported before being depleted in desorbable Ag_P (e.g. during floods), which may partially mask the contribution of intra estuarine Ag sources. In fact, historical records of Ag bioaccumulation in oysters from the estuary mouth (Lanceleur et al. 2011b) clearly suggest a growing influence of Ag from recent sources such as urban wastewater and cloud seeding. Because these potential sources are (at least partly) intra-estuarine (e.g. the Bordeaux agglomeration and vineyards on the Gironde Estuary banks), further work must aim at quantifying their part in the estuarine Ag budget and pollution.

Conclusion

In the salinity gradient of the Gironde Estuary, Ag_P in river-borne SPM decreased by 60–67 % due to chloride-induced desorption. This fraction is similar to the potentially bio-available, short-term reactive fraction as assessed by selective extraction (Ag_{HCl}), suggesting that the SPM average residence time in the estuary (1–2 years) allows complete desorption of the reactive Ag fraction. Silver-depleted SPM from the estuary mouth showed Ag_P/Th_P 0.019–0.028 during intermediate discharge, which is similar or lower than values in sediment from the West Gironde Mud Patch (Ag_P/Th_P 0.027 ± 0.001) and the geochemical background of the Gironde watershed (Ag_P/Th_P 0.024–0.028; Lanceleur et al. 2011a). Higher values (Ag_P/Th_P 0.040) during a flood suggest that exportation of non-depleted particles may result in Ag desorption in the coastal ocean and in the adjacent oyster farming areas in the Marennes-Oléron Bay. The Ag partitioning in the estuary reflects the balance between adsorption and desorption, i.e. by both salinity and SPM concentration, with minimum Ag_D in the MTZ and maximum levels (6–9 times greater than minimum Ag_D) in the mid-salinity range. Filter-passing (<0.2 μm) non-labile metal-organic Ag complexes assessed by solid-liquid extraction with and without previous UV treatment were not detectable in the MTZ and were highly variable in the mid/high salinity range (S020–33) where they accounted for up to 67 % (typically 10 to 50 %; average 28 %) of total dissolved Ag (UV-Ag_D).

Different approaches provided the first estimates of Ag_D net fluxes during the three cruises (flood 5.0 g/day; intermediate discharge ~1.7 g/day) and at the annual time scale (0.64–0.89 t/year in 2008 and 0.56–0.77 t/year in 2009). The first tentative Ag budget for the whole Gironde Estuary clearly showed that further work is necessary to understand the contribution of probable intra-estuarine Ag sources (e.g. Bordeaux urban agglomeration and agricultural activities).

References

Abril G, Etcheber H, Le Hir P, Bassoullet P, Boutier B, Frankignoulle M (1999) Oxic/anoxic oscillations and organic carbon mineralization in an estuarine maximum turbidity zone (The Gironde, France). Limnol Oceanogr 44:1304–1315

Abril G, Nogueira M, Etcheber H, Cabeçadas G, Lemaire E, Brogueira MJ (2002) Behaviour of organic carbon in nine contrasting European estuaries. Estuar Coast Shelf Sci 54:241–262

Audry S, Blanc G, Schäfer J, Chaillou G, Robert S (2006) Early diagenesis of trace metals (Cd, Cu, Co, Ni, U, Mo, and V) in the freshwater reaches of a macrotidal estuary. Geochim Cosmochim Acta 70:2264–2282

Audry S, Schäfer J, Blanc G, Bossy C, Lavaux G (2004) Anthropogenic components of heavy metal (Cd, Zn, Cu, Pb) budgets in the Lot-Garonne fluvial system (France). Appl Geochem 19:769–786

Ayrault S, Rianti Priadi C, Evrard O, Lefèvre I, Bonté P (2010) Silver and thallium historical trends in the Seine River basin. J Environ Monit 12:2177–2185

Barriada JL, Tappin AD, Evans HE, Achterberg EP (2007) Dissolved silver measurements in seawater. Trends Anal Chem 26:809–817

Barriada JL, Truscott JB, Achterberg EP (2003) Automation of a flow injection system for the determination of dissolved silver at picomolar concentrations in seawater with inductively coupled plasma mass spectrometry. J Autom Method Manag 25:93–100

Batley GE, Florence TM (1976) Determination of the chemical forms of dissolved cadmium, lead and copper in seawater. Mar Chem 4:347–363

Boyle EA, Collier R, Dengler AT, Edmond JM, Ng AC, Stallard RF (1974) On the chemical mass-balance in estuaries. Geochim Cosmochim Acta 38:1719–1728

Boyle EA, Huested SS, Grant B (1982) The chemical mass balance of the Amazon plume-II. Copper, nickel and cadmium. Deep-Sea Res 29:1355–1364

Bryan GW, Langston WJ (1992) Bioavailability, accumulation and effects of heavy metals in sediments with special reference to United Kingdom estuaries: a review. Environ Pollut 76:89–131

Castaing P, Allen GP (1981) Mechanisms controlling seaward escape of suspended sediment from the Gironde: a macrotidal estuary in France. Mar Geol 40:101–118

Castelle S, Schäfer J, Blanc G, Audry S, Etcheber H, Lissalde J-P (2007) 50-year record and solid state speciation of mercury in natural and contaminated reservoir sediment. Appl Geochem 22:1359–1370

Chiffoleau J-F, Auger D, Roux N, Rozuel E, Santini A (2005) Distribution of silver in mussels and oysters along the French coasts: data from the national monitoring program. Mar Pollut Bull 50:1719–1723

Ciffroy P, Garnier J-M, Benyahya L (2003) Kinetic partitioning of Co, Mn, Cs, Fe, Ag, Zn and Cd in fresh waters (Loire) mixed with brackish waters (Loire estuary): experimental and modelling approaches. Mar Pollut Bull 46:626–641

Comans RNJ, van Dijk CPJ (1988) Role of complexation processes in cadmium mobilization during estuarine mixing. Nature 336:151–154

Coynel A, Schäfer J, Blanc G, Bossy C (2007) Scenario of particulate trace metal and metalloid transport during a major flood event inferred from transient geochemical signals. Appl Geochem 22:821–836

Dabrin A, Schäfer J, Blanc G, Strady E, Masson M, Bossy C, Castelle S, Girardot N, Coynel A (2009) Improving estuarine net flux estimates for dissolved cadmium export at the annual timescale: application to the Gironde Estuary. Estuar Coast Shelf Sci 84:429–439

Davis JA (1977) Adsorption of trace metals and complexing ligands at the oxide/water interface. PhD thesis, Stanford University, Stanford, California, pp 176

Eisler R (1996) Silver hazards to fish, wildlife, and invertebrates: a synoptic review. Biol Sci Rep 32:44

Engel DW, Sunda WG, Fowler BA (1981) Factors affecting trace metal uptake and toxicity to estuarine organisms. I. Environmental parameters. In: Vernberg F, Calabrese A, Thurberg FP, Vernberg WB (eds) Biological monitoring of marine pollutants. Academic, New York, pp 127–144

Etcheber H, Taillez A, Abril G, Garnier J, Servais P, Moatar F, Commarieu MV (2007) Particulate organic carbon in the estuarine turbidity maxima of the Gironde, Loire and Seine estuaries: origin and lability. Hydrobiologia 588:245–259

Flegal AR, Brown CL, Squire S, Ross JRM, Scelfo GM, Hibdon S (2007) Spatial and temporal variations in silver contamination and toxicity in San Francisco Bay. Environ Res 105:34–52

Gobeil C, Rondeau B, Beaudin L (2005) Contribution of municipal effluents to metal fluxes in the St. Lawrence River. Environ Sci Technol 39:456–464

Holm-Hansen O, Lorenzen CJ, Holmes RW, Strickland JDH (1965) Fluorometric determination of chlorophyll. J Cons Int Explor Mer 30:3–15

Hornberger MI, Luoma SN, Cain DJ, Parchaso F, Brown CL, Bouse RM, Wellise C, Thompson JK (2000) Linkage of bioaccumulation and biological effects to changes in pollutant loads in South San Francisco Bay. Environ Sci Technol 34:2401–2409

Irigoien X, Castel J (1997) Light limitation and distribution of chlorophyll pigments in a highly turbid estuary: the Gironde estuary (SW France). Estuar Coast Shelf Sci 44:507–517

Jouanneau JM, Latouche C (1981) The Gironde Estuary. In: Fürchtbauer H, Lisitzyn AP, Millerman JD, Seibold E (eds) Contribution to sedimentology. E. Schweizerbart'sche Verlagsbuch-handlung, Stuttgart, pp 1–115

Lanceleur L, Schäfer J, Bossy C, Coynel A, Larrose A, Masson M, Blanc G (2011a) Silver fluxes to the Gironde Estuary—11 years (1999–2009) of monitoring at the watershed scale. Appl Geochem 26:797–808

Lanceleur L, Schäfer J, Chiffoleau J-F, Blanc G, Auger D, Renault S, Baudrimont M, Audry S (2011b) Long-term records of cadmium and silver contamination in sediments and oysters from the Gironde fluvial-estuarine continuum—evidence of changing silver sources. Chemosphere 85:1299–1305

Langston WJ, Burt GR, Pope ND (1999) Bioavailability of metals in sediments of the Dogger Bank (central North Sea): a mesocosm study. Estuar Coast Shelf Sci 48:519–540

Larrose A, Coynel A, Schäfer J, Blanc G, Masse L, Maneux E (2010) Assessing the current state of the Gironde Estuary by mapping priority contaminant distribution and risk potential in surface sediment. Appl Geochem 25:1912–1923

Lemaire E, Blanc G, Schäfer J, Coynel A (2006) Dissolved trace metal-organic complexes in the Lot-Garonne River system determined by the C18 Sep-pak system. Aquat Geochem 12:21–38

Luoma SN, Bryan GW (1981) A statistical assessment of the form of trace metals in oxidized surface sediments employing chemical extractants. Sci Total Environ 17:165–196

Luoma SN, Ho YB, Bryan GW (1995) Fate, bioavailability and toxicity of Ag in estuarine environments. Mar Pollut Bull 31:44–54

Masson M, Blanc G, Schäfer J (2006) Geochemical signals and source contributions to heavy metal (Cd, Zn, Pb, Cu) fluxes into the Gironde Estuary via its major tributaries. Sci Total Environ 370:133–146

Morford JL, Kalnejais LH, Helman P, Yen G, Reinard M (2008) Geochemical cycling of silver in marine sediments along an offshore transect. Mar Chem 110:77–88

Morse JW, Luther GW III (1999) Chemical influences on trace metal-sulfide interactions in anoxic sediments. Geochim Cosmochim Acta 63:3373–3378

Ndung'u K, Thomas MA, Flegal AR (2001) Silver in the western equatorial and South Atlantic Ocean. Deep-Sea Res II 48:2933–2945

Ndung'u K, Ranville MA, Franks RP, Flegal AR (2006) On-line determination of silver in natural waters by inductively-coupled plasma mass spectrometry: influence of organic matter. Mar Chem 98:109–120

Ratte HT (1999) Bioaccumulation and toxicity of silver compounds: a review. Environ Toxicol Chem 18:89–108

Rivera-Duarte I, Flegal AR (1997) Pore-water silver concentration gradients and benthic fluxes from contaminated sediments of San Francisco Bay, California, U.S.A. Mar Chem 56:15–26

Rivera-Duarte I, Flegal AR, Sañudo-Wilhelmy SA, Veron AJ (1999) Silver in the far North Atlantic Ocean. Deep-Sea Res II 46:979–990

Rodriguez Martin-Doimeadios RC, Monperrus M, Krupp E, Amouroux D, Donard OFX (2003) Using speciated isotope dilution with GC-inductively coupled plasma MS to determine and unravel the artificial formation of monomethylmercury in certified reference sediments. Anal Chem 75:3202–3211

Rozan TF, Hunter KS (2001) Effects of discharge on silver loading and transport in the Quinnipiac River, Connecticut. Sci Total Environ 279:195–205

Sañudo-Wilhelmy SA, Flegal AR (1992) Anthropogenic silver in the southern California Bight: a new tracer of sewage in coastal waters. Environ Sci Technol 26:2147–2151

Schäfer J, Blanc G (2002) Relationship between ore deposits in river catchments and geochemistry of suspended particulate matter from six rivers in southwest France. Sci Total Environ 298:103–118

Schäfer J, Blanc G, Lapaquellerie Y, Maillet N, Maneux E, Etcheber H (2002) Ten-year observation of the Gironde tributary fluvial system: fluxes of suspended matter, particulate organic carbon and cadmium. Mar Chem 79:229–242

Schmidt S, Tronczynski J, Guiot N, Lefevre I (2005) Dating of sediments in the Biscay bay: implication for pollution chronology. Radioprotection 40:655–660

Smith GJ, Flegal AR (1993) Silver in San Francisco Bay estuarine waters. Estuar Coasts 16:547–558

Sottolichio A, Castaing P (1999) A synthesis on seasonal dynamics of highly concentrated structures in the Gironde Estuary. C R Acad Sci II A 329:795–800

Strady E, Blanc G, Baudrimont M, Schäfer J, Robert S, Lafon V (2011) Roles of regional hydrodynamic and trophic contamination in cadmium bioaccumulation by pacific oysters in the Marennes-Oléron Bay (France). Chemosphere 84:80–90

Tappin AD, Barriada JL, Braungardt CB, Evans EH, Patey MD, Achterberg EP (2010) Dissolved silver in European estuarine and coastal waters. Water Res 44:4204–4216

U.S. EPA (Environmental Protection Agency) (2002) National recommended water quality criteria: 2002. EPA 882-R-02-047. Washington, DC: U. S. E.P.A., pp. 33. Available at: http://www.epa.gov/waterscience/criteria/wqcriteria.html

Van Calsteren P, Thomas L (2006) Uranium-series dating applications in natural environmental science. Earth Sci Rev 75:155–175

Wen L-S, Santschi PH, Gill GA, Paternostro CL, Lehman RD (1997) Colloidal and particulate silver in river and estuarine water of Texas. Environ Sci Technol 31:723–731

Wu F, Cai Y, Evans D, Dillon P (2004) Complexation between Hg(II) and dissolved organic matter in stream waters: an application of fluorescence spectroscopy. Biogeochemistry 71:339–351

Yang L, Sturgeon RE (2002) On-line determination of silver in seawater and marine sediment by inductively coupled plasma mass spectrometry. J Anal At Spectrom 17:88–93

Zhang Y, Obata H, Gamo T (2008) Silver in Tokyo Bay estuarine waters and Japanese rivers. J Oceanogr 64:259–265